

Imaging of multiple reflections

A. J. Berkhout¹ and D. J. Verschuur²

ABSTRACT

Current multiple-removal algorithms in seismic processing use either differential moveout or predictability. If the differential moveout between primaries and multiples is small, prediction is the only option available. In the last decade, multidimensional prediction-error filtering by weighted convolution, such as surface-related multiple elimination (SRME), have proved to be very successful in practice. So far, multiples have been considered as noise and have been discarded after the removal process. In this paper, we argue that multiple reflections contain a wealth of information that can be used in seismic processing to improve the resolution of reservoir images beyond current capability. In the near future, one may expect that the so-called weighted-crosscorrelation (WCC) concept may offer an attractive alternative in approaching the multiple problem. WCC creates an option to avoid the adaptive subtraction process as applied in prediction-error algorithms. Moreover, it allows the transformation of multiples into primaries. The latter means that seismic imaging with primaries and multiples (nonlinear process) can be implemented by a sequence of linear processes, including the transformation of multiples into primaries and the imaging of primaries.

INTRODUCTION

In the history of multiple removal, algorithms have been based on two differentiating properties: moveout and predictability. If primaries and multiples show different moveout behavior, algorithms are available that allow separation of primaries and multiples in a transform domain. Successful moveout-based methods use the Radon transform (Hampson, 1986; Herrmann et al., 2000; Trad et al., 2003). A weak point of moveout algorithms is that they are less effective in the situation of complex wavefields (e.g., nonhyperbolic

wavefronts). Moreover, these algorithms start to fail when the moveouts of primaries and multiples approach each other (e.g., with reflections from deep targets).

Predictability always has been an important property in multiples removal. In the early days of seismic processing (the 1960s), single-trace statistical prediction was successful (Robinson, 1957; Robinson and Treitel, 1980). In the early 1980s multichannel prediction-error filtering was given a wave-theoretical base, providing a unified theory for surface-related and internal multiples (Berkhout, 1982). The resultant feedback model gives physical insight into the multiple-scattering problem. Its main characteristic is that the seismic data themselves act as the multichannel prediction-error filter, a clear advantage in the situation of complex subsurface scattering mechanisms. At the surface, the measured seismic responses can be used as a secondary source to predict the surface multiples (Verschuur, 1991, 1992). Kelamis and Verschuur (2000) and Kelamis et al. (2002) also showed successful applications on land data. Now, multiple-removal algorithms to a large extent are presented as multichannel prediction-error filters that are explicitly or implicitly based on feedback (Wegein et al., 1997; Jakubowicz, 1998; Ikelle and Amundsen, 2002).

Recently, an alternative direction in the theory of multiple removal was proposed that is inspired by the double-focusing process as it occurs in bifocal seismic migration (Berkhout, 1997). The new theory is based on the focal transform (Berkhout, 2003; Berkhout et al., 2004). Application of the forward focal transform represents weighted crosscorrelation (WCC) and transforms primary energy into its focal point around zero time. After an imaging step, the result is input to the inverse focal transform, leading to the desired multiple-free output. Initial results indicate that combined weighted convolution and weighted crosscorrelation may lead to new opportunities in multiples removal.

The forward focal transform involves a correlation process of wavefields. In that respect, it is related to research carried out by Sun (2001), Schuster et al. (2004), and Wapenaar et al. (2004) in the area of so-called *daylight imaging*, described initially by Claerbout (1968) and more recently by Rickett and Claerbout (1999); however,

Manuscript received by the Editor April 8, 2005; revised manuscript received November 29, 2005; published online August 17, 2006.

¹Delft University of Technology, Faculty of Technology, Policy and Management, Delft, P.O. Box 5015, 2600 GA, Delft, The Netherlands. E-mail: a.j.berkhout@tbm.tudelft.nl.

²Delft University of Technology, Faculty of Applied Sciences, Laboratory of Acoustical Imaging and Sound Control, P.O. Box 5046, 2600 GA Delft/Lorentzweg 1, 2628 CJ, Delft, The Netherlands. E-mail: d.j.verschuur@tnw.tudelft.nl.

© 2006 Society of Exploration Geophysicists. All rights reserved.

a principal difference between the work of those authors and our approach is that we replace multichannel autocorrelation with multichannel crosscorrelation to avoid undesirable cross terms in the output. In addition, we refer to methods for imaging multiples that are based on an accurate earth model and the two-way wave equation (see, e.g., Reiter et al., 1991, and Youn and Zhou, 2001). A fundamental problem with these methods is the high accuracy of the required velocity field, including position and strength of the involved reflection boundaries (“the answer”). Moreover, Berkhout and Verschuur (1995), Guitton (2002), and Muijs et al. (2005) have proposed using the one-way wave equation to migrate multiple reflections. Here, a fundamental problem is that the source wavefield is very complex, which means that the traditional imaging condition cannot be used.

In this paper, we extend the theory of surface-related multiples — forward prediction by weighted convolution (SRME1) — and formulate it as a backward prediction process by weighted correlation. We demonstrate that this results in an attractive alternative for multiples removal (SRME2) as well as provides a mechanism to transform multiples into primaries (WCC). Combining all three algorithms allows implementation of nonlinear inversion by a series of linear steps. After describing the theory, we show the application of SRME2 for a synthetic data set from a seven-reflector model, where an improved multiple subtraction is obtained. Finally, we demonstrate the transformation of multiples into primaries for a synthetic data set from a 2D model with a salt layer, which leads to an increase in resolution of the subsurface image.

REMOVAL OF SURFACE-RELATED MULTIPLES: THE WEIGHTED-CONVOLUTION APPROACH

This section reviews the theory of data-driven surface-related multiples prediction. The so-called “feedback model” shows that prediction of multiples requires a weighted-convolution process with the primary response, the weighting function being determined by surface-related quantities (Berkhout, 1982, p. 211–218). If a rough estimate of the primary response is available, the convolution process becomes iterative. The convergence turns out to be fast, even if one starts with the total data set as the primary estimate.

Let us start with the feedback model (Figure 1), using the detail-hiding operator notation (see Appendix A):

$$\mathbf{P} = \Delta\mathbf{P} + \mathbf{M} = \Delta\mathbf{P} + \Delta\mathbf{P}\mathbf{A}\mathbf{P} \quad (1a)$$

or

$$\Delta\mathbf{P} = \mathbf{P} - \Delta\mathbf{P}\mathbf{A}\mathbf{P}. \quad (1b)$$

In equations 1a and 1b, \mathbf{P} represents the data volume with surface-related multiples, $\Delta\mathbf{P}$ represents the data volume without surface-related multiples, and \mathbf{M} represents the surface-related multiples. The expression $\mathbf{M} = \Delta\mathbf{P}\mathbf{A}\mathbf{P}$ shows that multiples are predicted by multiplying data matrix \mathbf{P} by operator matrix $\Delta\mathbf{P}\mathbf{A}$. If we bear in mind that one column of data matrix \mathbf{P} contains one frequency component of a shot record and that one row of data matrix $\Delta\mathbf{P}$ contains a receiver gather (Appendix A), then $\Delta\mathbf{P}\mathbf{A}\mathbf{P}$ represents weighted convolution, the weighting factors being given by surface-related matrix \mathbf{A} . The operator \mathbf{A} includes the free-surface reflectivity operator \mathbf{R}^\cap and compensates for source and detector properties as well, i.e., $\mathbf{A} = \mathbf{S}^{-1}\mathbf{R}^\cap\mathbf{D}^{-1}$. Note that the j th column of source matrix \mathbf{S} represents the source array at spatial position j , and the i th row of detector

matrix \mathbf{D} represents the detector array at spatial position i (see Appendix A).

Using the series expansion

$$\Delta\mathbf{P} = \mathbf{P} - (\mathbf{P}\mathbf{A})\mathbf{P} + (\mathbf{P}\mathbf{A})^2\mathbf{P} - (\mathbf{P}\mathbf{A})^3\mathbf{P} + \dots, \quad (2a)$$

an iterative version can be derived (Berkhout and Verschuur, 1997),

$$\Delta\mathbf{P}^{(n)} = \mathbf{P} - \Delta\mathbf{P}^{(n-1)}\mathbf{A}\mathbf{P}, \quad (2b)$$

where $\Delta\mathbf{P}^{(0)} = \mathbf{P}$ ($n = 1, 2, \dots$).

Equation 1b can be rewritten in terms of prediction-error filtering:

$$\Delta\mathbf{P} = \mathbf{P} - \mathbf{F}_{pr}\mathbf{P}, \quad \text{with } \mathbf{F}_{pr} = \Delta\mathbf{P}\mathbf{A}, \quad (3a)$$

or, using the iterative version 2b,

$$\Delta\mathbf{P}^{(n)} = \mathbf{P} - \mathbf{F}_{pr}^{(n)}\mathbf{P}, \quad \text{with } \mathbf{F}_{pr}^{(n)} = \Delta\mathbf{P}^{(n-1)}\mathbf{A}. \quad (3b)$$

The feedback model reveals that the prediction filter is a weighted version of the primary response, i.e., $\Delta\mathbf{P}\mathbf{A}$. This shows that multichannel prediction filters can be complicated. Considering that each column of $\Delta\mathbf{P}$ represents one shot record, the feedback model also shows that each output trace needs its own multichannel prediction filter that is derived from a range of shot records. This explains the failure of multichannel statistical filters that are based on one shot record.

In our algorithm for prediction-error filtering (SRME1), we use equation 3b and carry out in each iteration subtraction in the least-squares sense:

$$\mathbf{M}^{(n)} = \Delta\mathbf{P}^{(n-1)}\mathbf{A}\mathbf{P}, \quad \text{with } \mathbf{M}^{(0)} = 0 \quad (4a)$$

$$\Delta\mathbf{P}^{(n)} = \mathbf{P} - \mathbf{F}_{\ell_s}^{(n)}\mathbf{M}^{(n)}, \quad \text{with } \Delta\mathbf{P}^{(0)} = \mathbf{P}. \quad (4b)$$

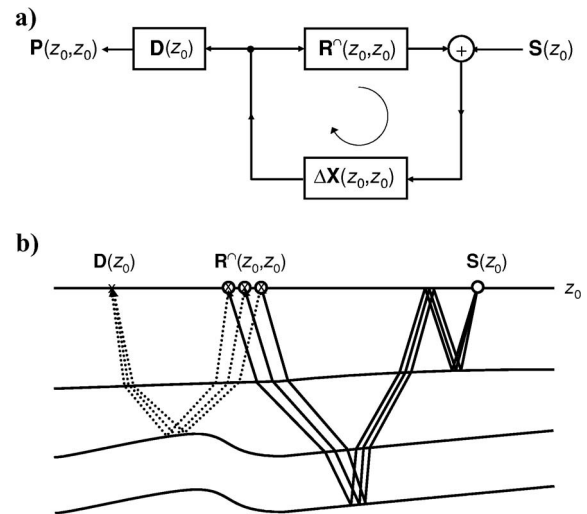


Figure 1. (a) Feedback model for primary reflections ($\Delta\mathbf{P}$) and data including surface-related multiples (\mathbf{P}), the multiple-generating boundary being given by $z_0 = z_0(x, y)$ and the downward-reflection operators of this boundary being represented by the columns of the matrix $\mathbf{R}^\cap(z_0, z_0)$. Here, $\mathbf{P} = \Delta\mathbf{P} + \Delta\mathbf{X}\mathbf{R}^\cap\mathbf{P}$ and $\Delta\mathbf{P} = \mathbf{D}\Delta\mathbf{X}\mathbf{S}$, where \mathbf{D} and \mathbf{S} represent the detector and source properties, respectively. (b) One basic element of the weighted convolution process for surface-related multiples (\mathbf{M}), visualized in terms of simple ray-paths, with $\mathbf{M} = \Delta\mathbf{X}\mathbf{R}^\cap\mathbf{P}$.

Experience with synthetic and field data (Verschuur and Berkhout, 1997; Miley et al., 2001) shows that, in practice, no more than three iterations are needed ($n \leq 3$).

Equations 4a and 4b demonstrate the advantage of introducing the wave-theoretical model (feedback model, Figure 1). Instead of estimating the complex prediction filter \mathbf{F}_{pr} , only the relatively simple adaption filter \mathbf{F}_{ls} needs to be computed (Verschuur, 1991). Using downward extrapolation, equations 1–4 can be extended to the removal of internal multiples (Berkhout 1982, p. 211–218; Berkhout and Verschuur, 2005).

REMOVAL OF SURFACE-RELATED MULTIPLES: THE WEIGHTED CROSSCORRELATION APPROACH

In this section, we demonstrate that the relations between primaries and multiples also can be rewritten as a weighted crosscorrelation. Therefore, once more we consider the feedback model (Figure 1a), as given by equation 1a:

$$\mathbf{P} = \Delta\mathbf{P} + \Delta\mathbf{P}\mathbf{A}\mathbf{P} \quad (5a)$$

or

$$\mathbf{P} = [\mathbf{I} - \Delta\mathbf{P}\mathbf{A}]^{-1}\Delta\mathbf{P}. \quad (5b)$$

Using the series expansion, this becomes

$$\mathbf{P} = \Delta\mathbf{P} + (\Delta\mathbf{P}\mathbf{A})\Delta\mathbf{P} + (\Delta\mathbf{P}\mathbf{A})^2\Delta\mathbf{P} + (\Delta\mathbf{P}\mathbf{A})^3\Delta\mathbf{P} + \dots, \quad (6a)$$

where $\Delta\mathbf{P}$ represents primaries, $(\Delta\mathbf{P}\mathbf{A})\Delta\mathbf{P}$ represents first-order multiples, and $(\Delta\mathbf{P}\mathbf{A})^2\Delta\mathbf{P}$ represents second-order multiples, etc. It can be observed from equation 6a that multiplying \mathbf{P} by the weighted primary operator $(\Delta\mathbf{P}\mathbf{A})$ transforms primaries into first-order multiples and first-order multiples into second-order multiples, etc.:

$$\mathbf{M} = \Delta\mathbf{P}\mathbf{A}\mathbf{P} = (\Delta\mathbf{P}\mathbf{A})\Delta\mathbf{P} + (\Delta\mathbf{P}\mathbf{A})^2\Delta\mathbf{P} + (\Delta\mathbf{P}\mathbf{A})^3\Delta\mathbf{P} + \dots \quad (6b)$$

In mathematical terms, multiplication with $(\Delta\mathbf{P}\mathbf{A})$ means weighted convolution, the weighting factors being given by matrix \mathbf{A} . Note that in this weighted-convolution process, all shot records are involved in computing one output trace. In physical terms, multiplication with $(\Delta\mathbf{P}\mathbf{A})$ means adding one round trip through the subsurface. This convolutional property has been used in our multiple-removal algorithm so far (SRME1), using the iterative version as given by equations 4a and 4b.

Now we will use operator $\Delta\mathbf{P}$ not in a convolution mode, but in a correlation mode, defining a so-called focal transform (see Berkhout and Verschuur, 2003; Berkhout et al., 2004):

$$\mathbf{Q} = \mathbf{F}\mathbf{P} \quad (\text{forward focal transform}) \quad (7a)$$

and

$$\hat{\mathbf{P}} = \mathbf{G}\mathbf{Q} \quad (\text{inverse focal transform}), \quad (7b)$$

with

$$\mathbf{G} = \Delta\mathbf{P} \quad (8a)$$

and

$$\mathbf{F} = \Delta\mathbf{P}^{-1} \approx \Delta\mathbf{P}^H\mathbf{B}, \quad (8b)$$

where

$$\mathbf{B} = (\Delta\mathbf{P}\Delta\mathbf{P}^H + \epsilon^2\mathbf{I})^{-1} \quad (\text{least-squares version}). \quad (8c)$$

In equation 8b, superscript H denotes the Hermitian operator, and in equation 8c, the extra term ϵ^2 is a small positive constant that we use for stabilization. Note that for a white reflection series, \mathbf{B} is determined by the directivity properties of source and detector arrays as used in the field. Thus, forward focal transformation means taking the seismic data with multiples to the focal domain using a multidimensional deconvolution (or WCC) with an estimate of the primary reflections. Inverse focal transform means going from the focal domain back to the original data domain. Application of the operator \mathbf{F} will transform the primary reflections into a band-limited focal point, first-order reflections into primaries, and second-order reflections into first-order reflections, etc.:

$$\begin{aligned} \mathbf{Q} &= \Delta\mathbf{P}^{-1}\mathbf{P} \approx \Delta\mathbf{P}^H\mathbf{B}\mathbf{P} \\ &= \hat{\mathbf{I}} + \hat{\mathbf{A}}\Delta\mathbf{P} + \hat{\mathbf{A}}(\Delta\mathbf{P}\mathbf{A})\Delta\mathbf{P} \\ &\quad + \hat{\mathbf{A}}(\Delta\mathbf{P}\mathbf{A})^2\Delta\mathbf{P} + \dots \end{aligned} \quad (9a)$$

or

$$\mathbf{Q} = \hat{\mathbf{I}} + \hat{\mathbf{A}}\mathbf{P}', \quad (9b)$$

with

$$\hat{\mathbf{I}} = \Delta\hat{\mathbf{P}}^{-1}\Delta\mathbf{P} \quad (\text{focal area}) \quad (9c)$$

and

$$\hat{\mathbf{A}} = \hat{\mathbf{I}}\mathbf{A} \quad (\text{weighted focal area}). \quad (9d)$$

In equations 9a–9d, matrices with a hat represent approximations. In mathematical terms, multiplication with $(\Delta\mathbf{P}^H\mathbf{B})$ indicates weighted crosscorrelation, the weighting factors being given by matrix \mathbf{B} . Note that in this WCC process, all shot records are involved in computing one output trace. In physical terms, multiplication with $(\Delta\mathbf{P}^H\mathbf{B})$ means removing one round trip through the subsurface. Matrix \mathbf{P}' represents the total response that has been recovered from the multiples:

$$\mathbf{P}' = [\Delta\mathbf{P}\mathbf{A}]^{-1}\mathbf{M}. \quad (10)$$

Equations 9a–9d are the theoretical base for a new concept in handling multiple scattering that involves separating primaries from multiples and transforming multiple reflections into primaries.

Separating primaries from multiples

Separating the band-limited energy around the focal point (at $t = 0$) from the other reflection energy and then applying inverse focal transformation obtains the primary response:

- Forward transformation:

$$\mathbf{Q} = \mathbf{F}\mathbf{P} = \hat{\mathbf{I}} + \hat{\mathbf{A}}\mathbf{P}', \quad \text{with } \mathbf{F} \approx \Delta\mathbf{P}^H\mathbf{B}. \quad (11a)$$

- Imaging step:

$$\Delta Q = \hat{\mathbf{I}} \quad (\text{focal area}), \quad (11b)$$

preferably in the τ - p domain to position all angle-dependent primary information at $\tau = 0$ (de Bruin et al., 1990).

- Inverse transformation:

$$\Delta P = G \Delta Q, \quad \text{with } G = \Delta \hat{P}. \quad (11c)$$

In the case of shallow water, the focal area and the deconvolved multiples are not well separated and imaging in the focal domain (equation 11b) needs to be carried out by least-squares subtraction in the focal domain:

$$\Delta Q = Q - F_{\ell_s} P. \quad (11d)$$

Note that F_{ℓ_s} yields an estimate of A .

Appendix B discusses strategies for combining surface-related multiple removal in the convolution and correlation modes.

Transforming multiple reflections into primaries

Transforming multiple reflections into primaries is an interesting application, as it opens a way to “transform noise into signal.” In addition, this new signal has the potential to fill in data that are missing because of acquisition gaps. Keep in mind that many recorded multiples are reflected by the surface at locations where detectors are not positioned. This effect becomes more favorable for higher-order multiples and may result in finely sampled primaries without interpolation:

$$Q = FP = \hat{I} + AP', \quad (12a)$$

$$X' \approx Q - \hat{I} = AP', \quad (12b)$$

which can be used as a new data set for surface-related multiple removal:

$$X' \rightarrow \Delta X' \quad (\text{SRME1} + \text{SRME2}). \quad (12c)$$

Here, X' represents the multidimensional unit impulse response of the subsurface that has been recovered from all multiples in P , and $\Delta X'$ represents the multidimensional unit primary impulse response of the subsurface that has been recovered from the first-order multiples in P (see also Appendix A). This multiple-based primary response now can be used for further processing. Thus, instead of reformulating a migration algorithm to handle multiple reflections directly, as proposed by Berkhout and Verschuur (1995), one transforms them into primaries first, then subjects them to the standard linear-migration process. Note that equation 12b is exact if X and S are Toeplitz matrices, which is the case for a 1D earth and a stationary source geometry.

The combination of all three modes of multiples removal is shown in Figure 2. The output of multiples mapped into primaries can be used to improve the input data by extending the aperture resulting from missing offsets. After that, the complete sequence can be applied again. In the next iteration, $\Delta X'$ is used to compute $\Delta X''$, where $\Delta X''$ is the multidimensional unit primary impulse response that has been recovered from the second-order multiples, etc. The combination of primary responses $\Delta X'$, $\Delta X''$, ... may be used to improve the migrated image, which currently is under investigation.

EXAMPLE OF MULTIPLE REMOVAL BY COMBINING WEIGHTED CONVOLUTION AND WEIGHTED CROSSCORRELATION

In the correlation mode, prediction and least-squares subtraction are replaced by focal transformation and imaging. This concept is demonstrated for reflection data that have been numerically simulated in a horizontally layered model with seven reflectors (see Figure 3). For this 1D subsurface model, the data matrix P has a Toeplitz structure (elements along a diagonal are equal) (see also Figure A-2a). In Figure 4a and b, the modeled shot record is displayed with and without surface multiples. Note that in Figure 4b, internal multiples still are present. Figure 4c displays the modeled surface-related multiples. It is well known that least-squares subtraction in the data domain is not guaranteed to realize the best multiple suppression but rather results in the section with the least energy. The leakage in adaptive subtraction has been reported by several authors (e.g., Nekut and Verschuur, 1998; Spitz, 2000; Guitton and Verschuur, 2004). This undesired property is demonstrated in Figure 5. We start with perfect multiples prediction, using the true primaries as the convolution operator, as described by equation 1b. The predicted multiples are adaptively subtracted from the true multiples, yielding a close-to-perfect output, as expected (Figure 5c). Next, these predicted multiples also are adaptively subtracted from the input data, yielding a result that is illustrative for the subtraction problems that are encountered in practice (Figure 5e). The difference between this subtraction result in Figure 5e and the modeled multiple-free data in Figure 4b shows a nonzero result (Figure 5f), indicating that even with perfectly predicted surface-related multiples, minimum-energy adaptive subtraction does not provide the best multiple-removal result. In Figures 5c and 5f, adaptive subtraction was carried out with a least-squares filter with a length of 40 ms, locally applied within overlapping windows of 800-ms length and with a 20-trace width.

For the imaging approach (SRME2), the focal transform is calculated from the input data (repeated in Figure 6a), using the primary estimate from SRME1 as the focal operator. Because we deal here with a 1D subsurface, P and ΔP are Toeplitz matrices and the least-squares calculation of ΔP^{-1} becomes a scalar division in the spatial

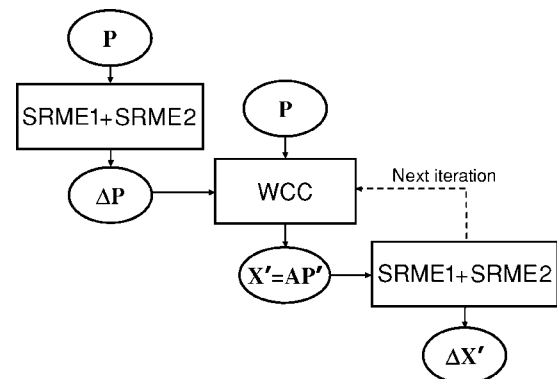


Figure 2. The output of SRME1 and SRME2 yields the estimated primaries ΔP , serving as operator for the WCC process. The output of WCC represents the total impulse response X' that is recovered from all multiples in P . Next, X' is used as input for a new SRME1 + SRME2 process. The output represents the primary impulse response $\Delta X'$ that is recovered from the first-order multiples in P . The combination of $\Delta X'$ and X' then can be used to recover the primary impulse response from the second-order multiples $\Delta X''$, etc.

Fourier domain. Bear in mind that application of the focal transform involves multichannel WCC. The resultant focal domain is displayed in Figure 6b. The primary energy is concentrated in the area around the origin ($t = 0$), and the surface-related multiples constitute a replica of the total data ($t > 0$). Next, the total data are adaptively subtracted in the focal domain (see equation 11d) to separate the primary energy that is around the origin from the other events. The result of this operation is displayed in Figure 6c. Figure 6e displays the linear Radon transform of the focal-domain data of Figure 6b. Note that the energy from the focal area now is visible as a horizontal event at $\tau = 0$. Hyperbolic events are visible as ellipses. After subtraction of the input data (Figure 6d), the result is displayed in Figure 6f. Finally, inverse focal transformation yields the new primary estimate (see Figure 7). Figure 7b shows the result of three iterations. The significant improvement with respect to SRME1 alone is clear (compare Figures 5f and 7c). Note that the focal transform reorganizes the locations of primary and multiple energy to minimize their overlap, which improves primary/multiple separation.

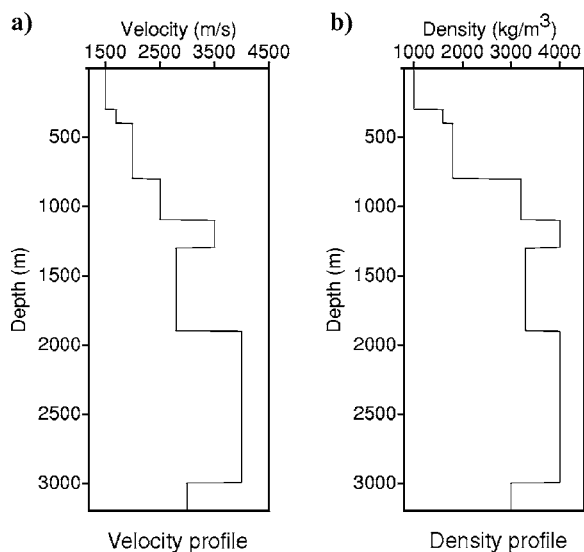


Figure 3. Vertical cross sections through a horizontally layered model with seven reflectors. (a) Velocity profile. (b) Density profile.

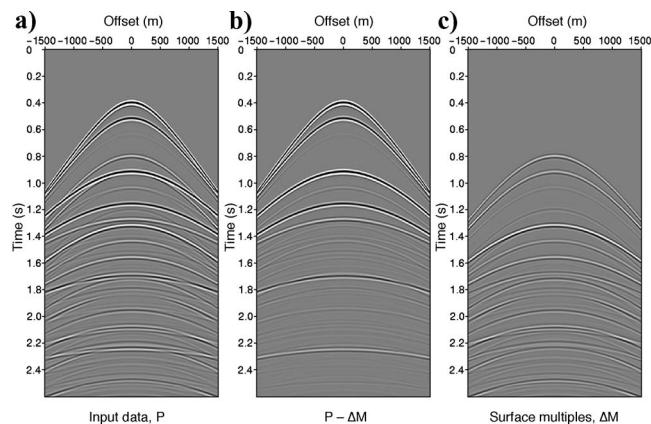


Figure 4. Data generated in the horizontally layered model with seven reflectors that are shown in Figure 3. (a) Shot record with all multiples. (b) Shot record with primaries plus internal multiples. (c) Shot record with surface multiples only.

EXAMPLE OF CONSTRUCTING PRIMARIES FROM MULTIPLES

The second application of focal transformation is the mapping of multiples into primaries such that the newly obtained primaries also can be used in imaging algorithms. Once multiples are transformed into primaries, all other processing steps that follow are the same as in traditional primary processing. This avoids the need to reformulate imaging algorithms for multiple scattering. Such was described by Berkhout and Verschuur (1995) and further illustrated by Guitton (2002). It is interesting that a similar reasoning can be found in seismic-data interpolation: When the offset distribution of irregularly sampled seismic data is regularized, all other processing steps can take advantage of algorithms for regular geometries.

To demonstrate the transformation of multiples into primaries, we consider a relatively complex subsurface model. Figure 8 shows the subsurface model that contains vertical and lateral velocity and density variations. The model is used to simulate seismic data with an acoustic finite-difference scheme. An anticlinal salt structure overlies the target — a fault structure — and strong surface-related multiples are expected that are related to the water bottom and the salt top.

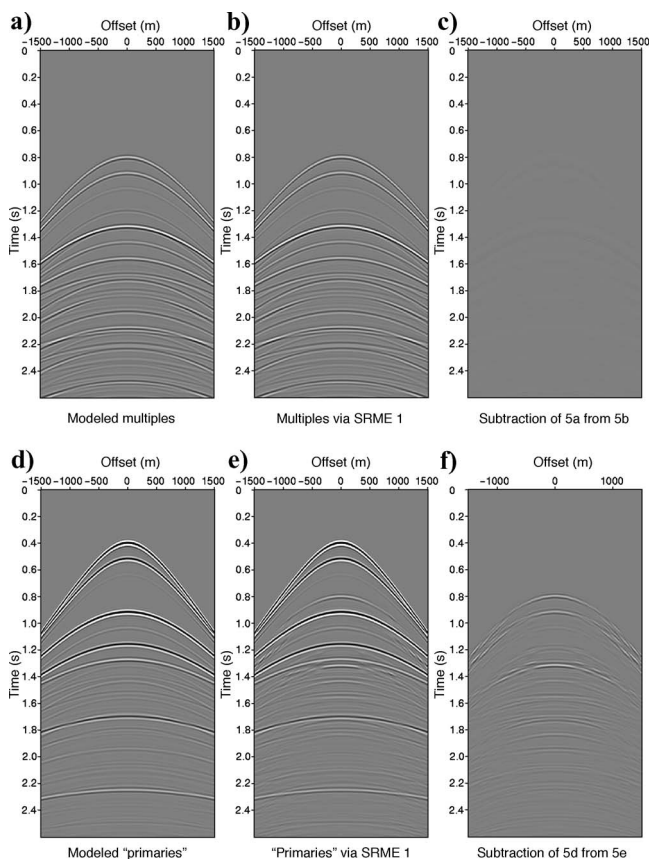


Figure 5. Leakage problem with least-squares subtraction, illustrated for the data in Figure 4. (a) Modeled surface multiples. (b) Predicted multiples via SRME1. (c) Least-squares subtraction from modeled multiples. (d) Modeled primaries with internal multiples ("primaries"). (e) Primaries obtained by least-squares subtraction of the predicted multiples via SRME1 from the input data. (f) Least-squares subtraction leakage. The difference between (c) and (f) shows that the imperfection of SRME1 is not in the prediction, but in the subtraction.

Data are modeled in a fixed-spread configuration, with sources and receivers positioned between $x = 0$ and $x = 5400$ m, with a step size of 15 m. This results in a prestack data set of 361×361 traces. For this example, the data matrix \mathbf{P} is far from Toeplitz (see Figure A-2b); hence, the least-squares inverse of $\Delta\mathbf{P}$ was computed with the aid of equations 8b and 8c. Note that each column of matrix $\Delta\mathbf{P}$ rep-

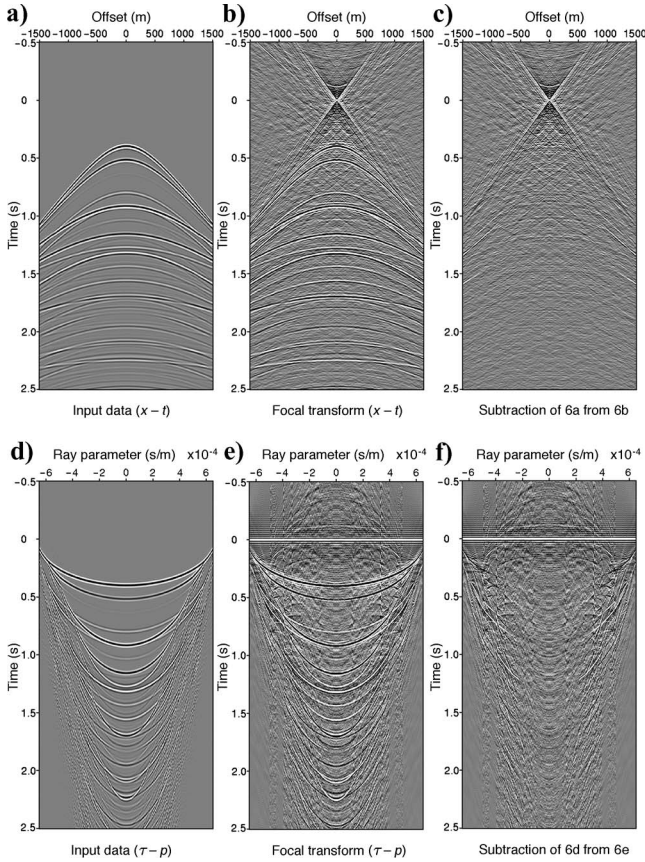


Figure 6. Multiple removal for the data in Figure 4a. (a) Input data with multiples. (b) Focal transform of input data, using the primary estimate of SRME1. (c) SRME2 output in the focal domain by adaptive subtraction in $x-t$. (d) Input data in $\tau-p$. (e) Focal transform of input data in the $\tau-p$ domain. (f) SRME2 output in the focal domain by adaptive subtraction in $\tau-p$.

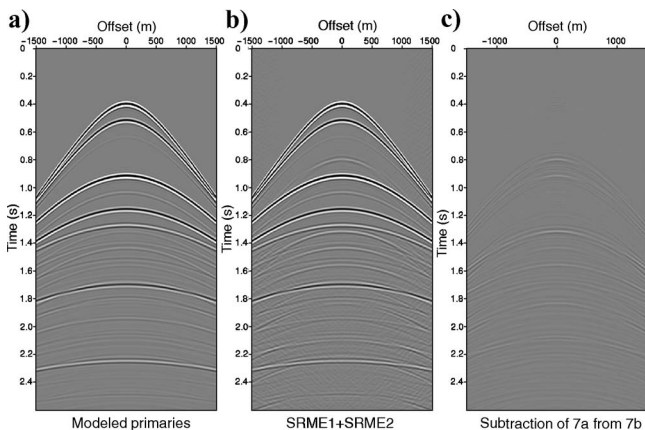


Figure 7. Multiple removal for the data in Figure 4a. (a) Modeled primaries. (b) Primaries obtained using three iterations of SRME1 + SRME2. (c) Difference between (a) and (b). Note the very small subtraction leakage compared to Figure 5f.

resents one frequency component of a shot record with 361 traces. To make the example more realistic, the band-limited version of a measured air-gun signature with a visible bubble was used for the source wavelet (see Figure 9). This information is contained in the source matrix \mathbf{S} . Figure 10 displays three shot records. The source locations are at $x = 750$ m, $x = 1500$ m, and $x = 2250$ m, respectively, the 2250-m value being located close to the top of the salt

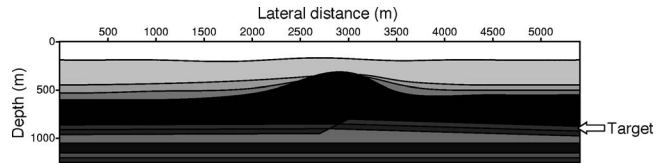


Figure 8. Subsurface model that contains a high-velocity salt layer that overlies the target area with a fault structure.

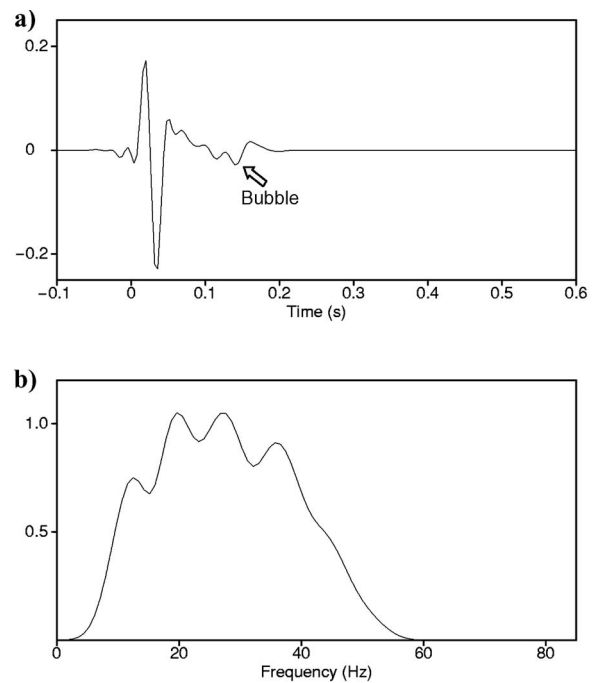


Figure 9. Band-limited version of a measured air-gun signature that was used in the data simulation. (a) Time-domain representation. (b) Amplitude spectrum.

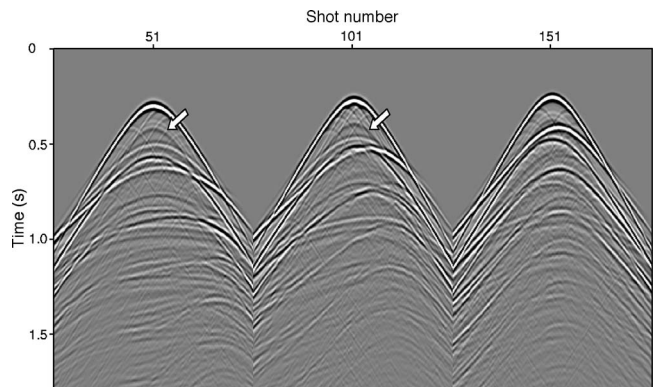


Figure 10. Three shot records — including all types of multiples — that were modeled in the subsurface model of Figure 8 and using the air-gun wavelet of Figure 9. Note the artificial reflection that comes from the bubble (see the arrows).

structure. Note the strong surface-related multiples that mask the target reflections from the fault structure below the salt layer.

First, the iterative surface-related multiple-removal scheme in the convolution mode (SRME1) is applied to these data. Three iterations appear sufficient for a good multiple attenuation. Note that in Figure 11, the primary reflections from the top of salt and the surrounding sediments, as well as the reflections from the target area below the salt, now are well visible. Note also the internal multiple between the water bottom and the top of salt, which is especially visible in shot record 151 at apex time 0.55 s.

Next, multidimensional focal transformation is applied to the input data with multiples, using the output of SRME1 as the focal operator. Bear in mind that application of the focal transform involves multichannel WCC with the SRME1 output, as described by equations 8b and 8c. Figure 12 shows the result for the three shot locations under consideration. The focal domain shows the expected characteristics: a large amount of energy in the focal point and a replica of the input data — being constructed from surface multiples — at the positive traveltimes. After muting the energy at and around the focal point, the new data with multiples, $\mathbf{X}' = \mathbf{A}\mathbf{P}'$, are displayed in Figure 13. It can be seen that all details with respect to diffractions at the water bottom and the involved complex multiple-reflection behavior have been captured well by the WCC process. The input data and the WCC result are compared for a common-offset section, the offset being 75 m. Figure 14a displays the common-offset traces from the original input data with multiples, and Figure 14b shows the same common-offset section selected from the WCC result. Note the significantly better resolution of the output of WCC; the lengthy air-gun wavelet (minimum phase) has been replaced by a short zero-phase wavelet. Because the output of WCC represents a new version of the total data set \mathbf{X}' , it can serve as input for an SRME1 + SRME2 process to remove the multiples (see also Figure 2). Figure 14d displays the resulting common-offset section after this procedure. Although the output suffers from some residual multiple energy compared to the output of SRME1 only (Figure 14c), the increase in temporal resolution still is present. It is important to realize that the resultant deconvolved primaries $\Delta\mathbf{X}'$ are recovered from first-order surface multiples. In a final comparison, the output of SRME1 and of WCC + SRME1 were prestack depth migrated. Figure 15 displays both results. Note again that the result of WCC + SRME1 yields much better vertical and lateral resolution. This

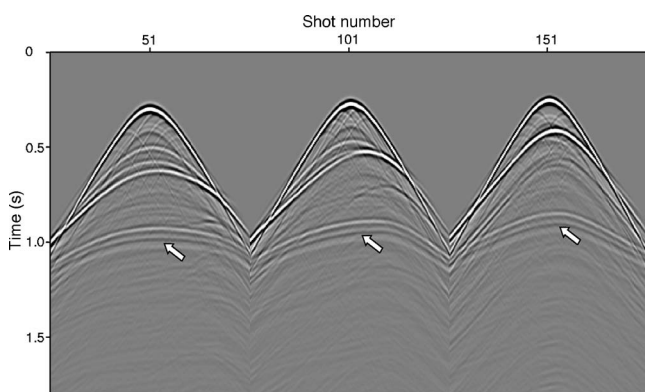


Figure 11. The three shot records of Figure 10 after three iterations of surface-related multiple removal using the convolution approach (SRME1). Note the enormous reduction in multiple energy and the revealing of the target reflections below the salt at approximately 1.0 seconds (see the arrows).

can be observed from the intersection of the two sediment layers and the flanks of the salt at approximately 500 m depth. Especially at the right-hand side (below lateral location 3300 m), the result of WCC + SRME1 is significantly sharper. Note also that the thin layer at 1200 m depth is much clearer in the result of WCC + SRME1; in the conventional depth migration, it appears as one reflector.

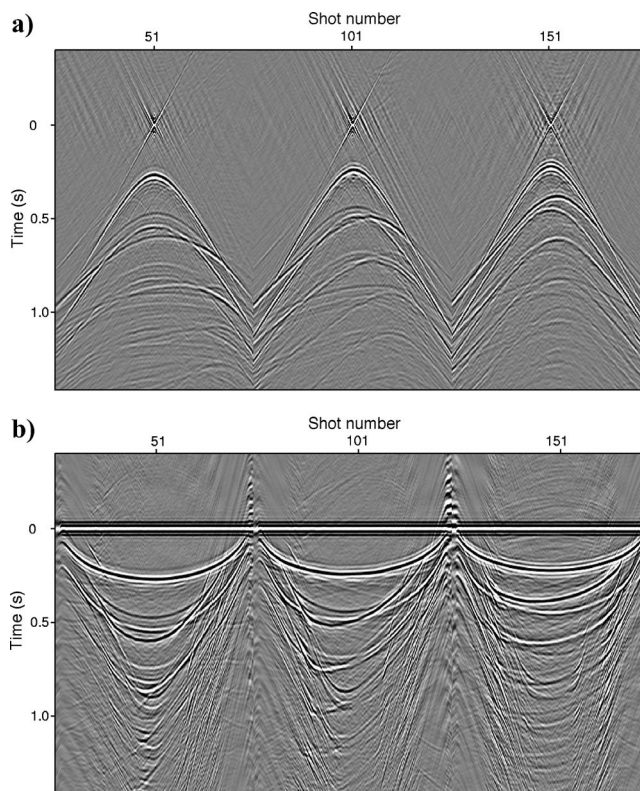


Figure 12. Focal transform of the data with multiples, using the SRME1 output as the multidimensional focal operator. The shot records are displayed for the same source locations as are used in Figures 10 and 11. (a) Presentation in the $x-t$ domain. (b) Presentation in the $\tau-p$ domain. Note that all primaries are mapped into the focal point at and around $t = 0$ and $\tau = 0$, respectively.

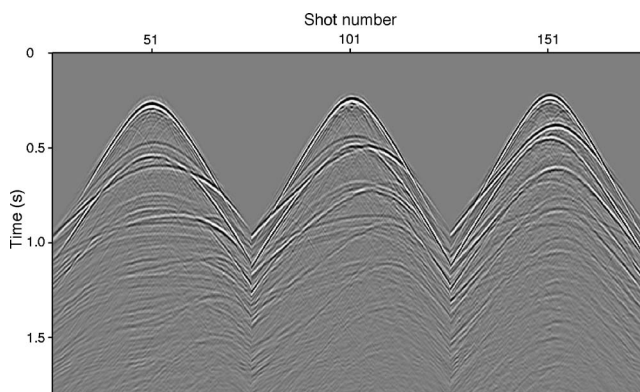


Figure 13. Three shot records obtained by removing the energy at the focal point in Figure 12a by removing the energy around $\tau = 0$ in Figure 12b thus creating a new data set of primaries and multiples from the recorded surface-related multiples ($\mathbf{X}' = \mathbf{A}\mathbf{P}'$). Note improved resolution with respect to the original input data in Figure 10.

DISCUSSION

Multiples removal by the combination of weighted convolution (SRME1) and weighted crosscorrelation (SRME2) now is being evaluated on different field data sets as part of DELPHI consortium research. The transformation of multiples into primaries (WCC) is being used to construct primaries at missing offsets from multiple scattering at available offsets. We expect that diffracted multiple re-

flections contain a wealth of information to fill in primary information that has not been recorded.

By transforming shot records into common-focus-point (CFP) gathers, sources at the surface are repositioned in the subsurface (Berkhout, 1997). This means that if we replace shot records with CFP gathers, the theory presented also is applicable to seismic responses at the surface that come from sources in the subsurface. Note that such reformulation in terms of CFP gathers still requires a focal-transform operator with both sources and detectors at the surface:

- 1) Prediction of multiples from recorded reflection data:

$$\mathbf{M}(z_0, z_s) = \Delta \mathbf{P}(z_0, z_0) \mathbf{A}(z_0, z_0) \mathbf{P}(z_0, z_s). \quad (13a)$$

- 2) Transformation of multiples into new reflection data:

$$\begin{aligned} \mathbf{X}'(z_0, z_s) \\ = \Delta \mathbf{P}^H(z_0, z_0) \mathbf{B}(z_0, z_0) \mathbf{M}(z_0, z_s). \end{aligned} \quad (13b)$$

In prediction equation 13a, a matrix $\mathbf{P}(z_0, z_s)$ represents reflection data — primaries and multiples — that are recorded at the surface z_0 from (virtual) sources at depth z_s . In transformation equation 13b, matrix $\mathbf{X}'(z_0, z_s)$ represents new reflection data that are created from the multiples. From equations 13a and 13b, note the weighted-convolution operator $\Delta \mathbf{P}(z_0, z_0) \mathbf{A}(z_0, z_0)$ and the WCC operator $\Delta \mathbf{P}^H(z_0, z_0) \mathbf{B}(z_0, z_0)$ are independent of source location. These operators only depend on where the recording takes place. In other words, active seismic measurements (i.e., recordings from man-made sources at the surface) are required to transform multiples into primaries from passive seismic measurements (i.e., recordings from natural sources in the subsurface) when

these sources are not fully uncorrelated (see, e.g., Wapenaar et al., 2004). This important observation is the basis of our current research.

CONCLUSIONS

Focal transformation — i.e., WCC of seismic-reflection data with an estimate of the primary response — opens new opportunities in seismic processing. This paper has shown two applications: (1) moving multiples by combining weighted convolution (SRME1) with weighted crosscorrelation (SRME2) and (2) transforming multiples scattering into primary reflections (WCC). It is expected that SRME2 will create an option to avoid the adaptive-subtraction process in prediction-error algorithms. It is also expected that the combination of SRME1 + SRME2 with WCC may lead to new insight in the processing of multiples scattering, particularly because reflected and diffracted multiple energy is contributing constructively to the final image.

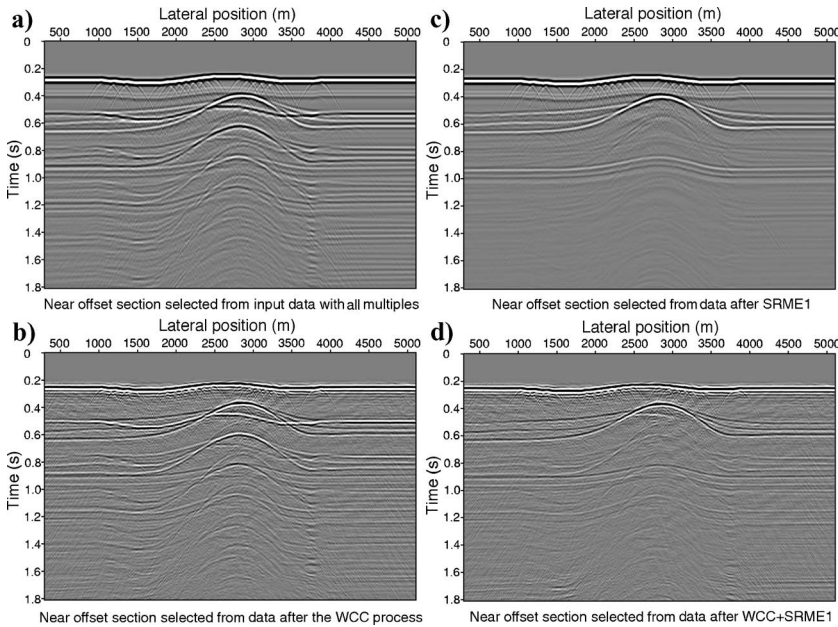


Figure 14. Transformation of multiples \mathbf{M} into deconvolved primaries $\Delta \mathbf{X}'$. (a) Near-offset section selected from the input data with all multiples \mathbf{P} . (b) Near-offset section selected from the output of the WCC process ($\mathbf{X}' = \Delta \mathbf{P}'$). (c) The near-offset section selected from the data after surface-multiple removal (SRME1). (d) The near-offset section from the WCC output after an additional SRME1 process. The WCC output contains all the details of the original data, such as the water-bottom diffractions. Furthermore, the data extracted from the multiples have a zero-phase characteristic, which leads to an increased vertical resolution.

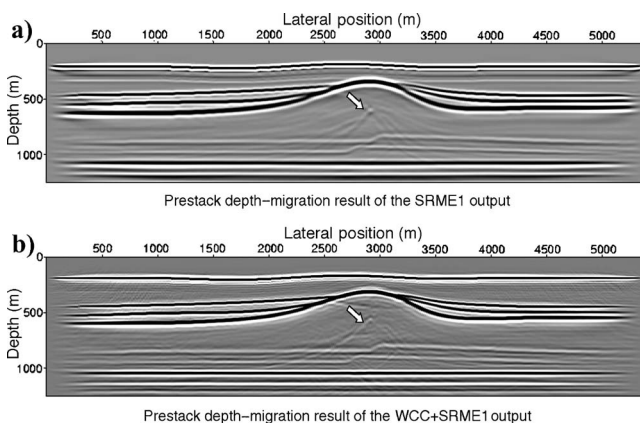


Figure 15. Migration of $\Delta \mathbf{P}$ and $\Delta \mathbf{X}'$. (a) Prestack depth migration result of the SRME1 output. (b) Prestack depth migration result of the WCC + SRME1 output, meaning that (b) represents the subsurface image of all first-order, surface-related multiples. Note again the improved vertical and horizontal resolution in (b) with respect to (a). Note that increase in resolution appears at the cost of an increase in background noise. The arrows point to internal multiple energy, which is not addressed by this procedure.

ACKNOWLEDGMENTS

The authors thank the sponsors of the DELPHI consortium for the support of this research and for the stimulating discussions at the consortium meetings. Furthermore, the authors thank the anonymous reviewers for their suggestions on improving the paper.

APPENDIX A

OPERATOR FORMULATION OF SEISMIC DATA

The data of a seismic survey always are a discrete spatial sampling of the wavefield. Therefore, seismic data traces can be arranged conveniently in a so-called data matrix. After waves that have traveled along the surface have been removed, the data matrix contains signals that can be expressed in terms of wavefield operators that describe propagation and reflection in the subsurface.

The data matrix

It has been shown (Berkhout, 1982, 1993) that the data of a seismic survey (2D or 3D) can be arranged conveniently using the data matrix $\mathbf{P}(z_a, z_b)$ — a matrix of frequency-domain signals — where the (i, j) element represents one frequency component of the signal recorded by a receiver at lateral location i from a source at lateral location j , where the receiver and source depths are z_a and z_b , respectively (Figure A-1). This matrix can be used directly for the formulation of wave-theory-based numerical algorithms in seismic-signal processing such as multiples removal and prestack migration. Note that in most theoretical considerations, the data matrix is assumed to be filled completely with regularly sampled measurements. Figure A-1 illustrates that this is not the case in practice. During a seismic survey, not every surface location is occupied by both a source and a receiver, so that some elements of the matrix will be empty. For example, if only zero-offset data were collected, then the data matrix would be diagonal. Note also that in the frequency domain, each element of the data matrix represents the frequency component of a single trace, i.e., one complex number. Figure A-2 shows the data matrix

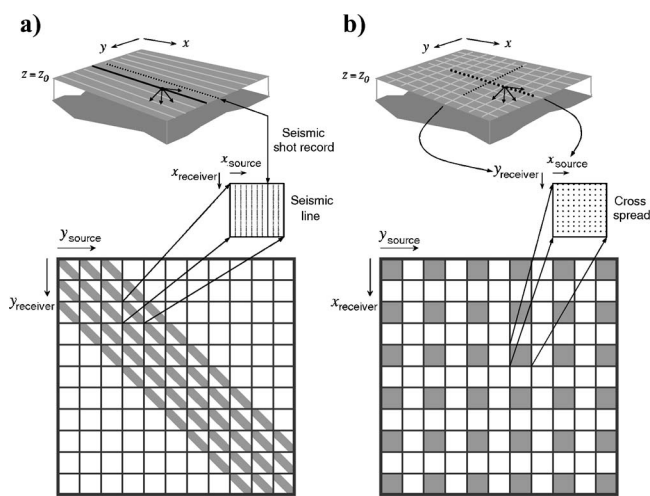


Figure A-1. The data matrix for 3D seismic measurements. In multi-streamer marine data (a), one column represents one shot record. (In this example, five streamers are shown.) In multicross-spread land data (b), one submatrix represents the data of a single cross-spread. (In this example, 36 cross-spreads are shown.)

matrix ($f = 30$ Hz) for the data of the seven-reflector model (see Figure 3) and the salt model (see Figure 8). Note the Toeplitz structure in Figure A-2a.

Source, transfer, and receiver matrices

The wave equation is linear and time invariant, so that the signal recorded by a receiver at the i th location from a source at the j th location may be written as the convolution of the source wavelet with a medium transfer function and a receiver impulse response. In the frequency domain, the data matrix may be written as the product

$$\mathbf{P}(z_0, z_0) = \mathbf{D}(z_0)\mathbf{X}(z_0, z_0)\mathbf{S}(z_0). \quad (\text{A-1})$$

In equation A-1, the j th column of the source matrix $\mathbf{S}(z_0)$ defines the downgoing source wavefield at surface z_0 when the source array is at position j . The (i, j) element of the transfer matrix $\mathbf{X}(z_0, z_0)$ defines the upgoing wavefield at location i that is produced by a unit source at location j (source and receiver both at the surface z_0), and the i th row of the receiver matrix $\mathbf{D}(z_0)$ gives the sensitivity of the i th seismic trace to the upgoing wavefield at surface z_0 when the receiver array is at location i . Thus, the (i, j) element of the data matrix $\mathbf{P}(z_0, z_0)$ is the seismic trace when the receiver array is at location i and the source array is at location j . In the special situation of single-point sources and single-point receivers (no arrays), \mathbf{S} and \mathbf{D} are diagonal matrices.

WRW model

While the full data matrix contains the raw measurements with surface-related and interbed multiples, the first goal of seismic processing commonly is to construct a new data matrix that contains only signals that go down to the target, reflect once, and return directly to the sensor, i.e., that is a single-scattering approximation to the full data matrix. This data matrix for single scattering $\Delta\mathbf{P}(z_0, z_0)$ can be expressed in terms of propagation and reflection operators according to

$$\Delta\mathbf{P}(z_0, z_0) = \mathbf{D}(z_0)\Delta\mathbf{X}(z_0, z_0)\mathbf{S}(z_0), \quad (\text{A-2a})$$

with

$$\Delta\mathbf{X}(z_0, z_0) = \sum_m \mathbf{W}(z_0, z_m)\mathbf{R}(z_m, z_m)\mathbf{W}(z_m, z_0) \quad (\text{A-2b})$$

for each Fourier (or Laplace) component (Figure A-3). The source matrix $\mathbf{S}(z_0)$ and receiver matrix $\mathbf{D}(z_0)$ in equation A-2a are the same as those encountered in equation A-1. In equation A-2b, the columns

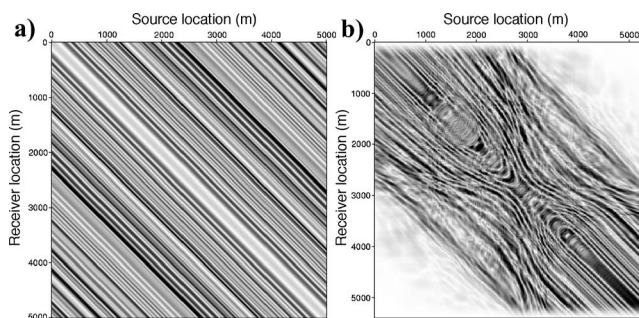


Figure A-2. Data-matrix representation for prestack data with all multiples that are related to one frequency of 30 Hz. (a) Data based on the seven-reflector model of Figure 3. (b) Data based on the salt model of Figure 8.

of $\mathbf{W}(z, z_0)$ are the (pseudo) primary propagation operators of the downgoing wavefield from each point at surface z_0 to every point at depth level z . Similarly, the columns of $\mathbf{W}(z_0, z)$ are the propagation operators of the upgoing wavefield from each point at depth z to every point at the surface z_0 . Because of the reciprocity principle, $\mathbf{W}(z, z_0) = \mathbf{W}(z_0, z)^T$, where superscript T means transpose. Each column of \mathbf{W} defines a unit point-source response, so that the elements of a single-arrival version may be written as

$$W_{\ell_j}(z_m, z_0) = a_{\ell_j}^+ e^{-j\omega\tau_{\ell_j}} H(\omega), \quad (\text{A-3a})$$

$$W_{ik}(z_0, z_m) = a_{ik}^- e^{-j\omega\tau_{ik}} H(\omega), \quad (\text{A-3b})$$

where $H(\omega)$ defines the spectrum of a band-limited temporal differentiator (optionally including fine-layering effects), τ_{ℓ_j} is the traveltime from the source point (x_j, z_0) to the reflection point (x_{ℓ_j}, z_m) , and τ_{ik} is the traveltime from the reflection point (x_k, z_m) to the detector point (x_i, z_0) . Here, $a_{\ell_j}^+$ and a_{ik}^- are related amplitude-attenuation factors that include geometrical spreading and transmission losses. Note that in the multiarrival version, a and τ are frequency dependent.

In equation A-2b, the reflection operator for the downgoing wavefield at depth z_m is $\mathbf{R}(z_m, z_m)$ (Figure A-3). If we take a diagonal matrix for \mathbf{R} , then the reflection process is angle-independent. Angle-dependent reflectivity can be represented by a nondiagonal matrix \mathbf{R} . For example, the plane-wave-reflection coefficient from a horizontal interface would be applied to an incoming wavefield as a scalar multiplication in the frequency-wavenumber domain. Our operator formalism represents signals in the frequency-space domain, where the multiplication in wavenumber may be expressed as a convolution in space by picking the appropriate form for \mathbf{R} (Berkhout, 1982; de Bruin et al., 1990; de Bruin, 1991).

Equation A-1b is a discrete implementation of continuous Kirchhoff-type integrals, describing propagation down, reflection, and propagation up (WRW). Note that for continuous 3D primary reflection

the evaluation of each element of $\Delta\mathbf{X}(z_0, z_0)$ involves two sets of double integrals per depth level. The first set of double integrals gives the reflected wavefield at depth z ,

$$\begin{aligned} \delta X(\mathbf{x}, z; \mathbf{x}_s, z_0; \omega) \\ = \int \int R(\mathbf{x}, z; \mathbf{x}', z; \omega) W(\mathbf{x}', z; \mathbf{x}_s, z_0; \omega) d^2 \mathbf{x}', \end{aligned} \quad (\text{A-4a})$$

for each source point (\mathbf{x}_s, z_0) that is related to the elements of $\mathbf{S}(z_0)$. The second set of double integrals propagates the reflected wavefield at depth z back to the receiver at the surface,

$$\begin{aligned} \delta X(\mathbf{x}_r, z_0; \mathbf{x}_s, z_0; \omega) \\ = \int dz \int \int W(\mathbf{x}_r, z_0; \mathbf{x}, z; \omega) \delta X(\mathbf{x}, z; \mathbf{x}_s, z_0; \omega) d^2 \mathbf{x}, \end{aligned} \quad (\text{A-4b})$$

for each receiver point (\mathbf{x}_r, z_0) that is related to the elements of $\mathbf{D}(z_0)$. The full signal then is composed by integrating over every depth slice of the reflectors. In equations A-4a and A-4b, any lateral position (x, y) has been indicated by the vector \mathbf{x} . Hence, the location of a gridpoint at lateral position k of depth level z_m is defined by (\mathbf{x}_k, z_m) . Note that in two dimensions, the vector \mathbf{x} needs to be replaced by the scalar x .

In the situation of multiples, the WRW model is extended with a feedback loop that represents up-down reflection (see Figure 1a). To distinguish between down-up and up-down reflection, we use the extended notation \mathbf{R}^U and \mathbf{R}^\cap , respectively.

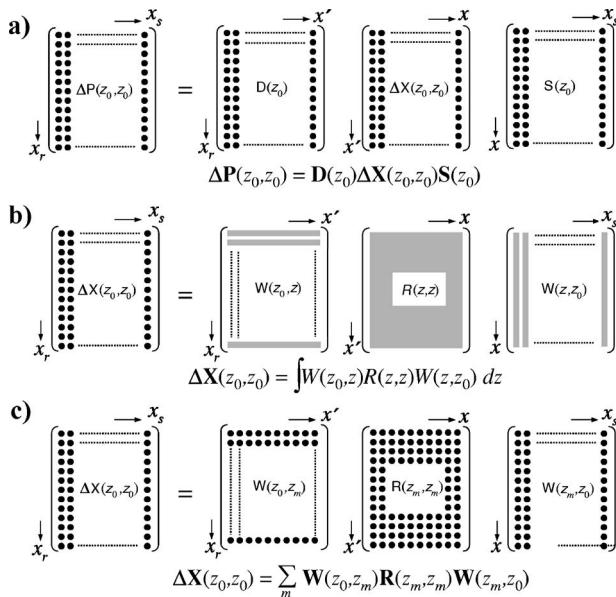


Figure A-3. Pictorial illustration of the 3D primary reflection model for the measurements (a) and the transfer function (b and c), the latter being based on the continuous (b) and the discrete (c) formulation of wave propagation.

Seismic data processing

The operator formulation yields a system view of seismic-wave theory. If the wavefield operators in the signal model are represented by matrices that have the predefined structure (Figures A-1 and A-3), then they also can be used to implement seismic-data-processing algorithms. For instance, multiplication of a primary seismic data set with the matrix operator \mathbf{W} defines a forward wavefield-extrapolation process in a heterogeneous subsurface, the extrapolation operator for lateral position \mathbf{x}_k being represented by the k th row of \mathbf{W} . Similarly, multiplication of a seismic data set with matrix operator \mathbf{R} defines an angle-dependent and frequency-dependent reflection process at any type of geological boundary, the reflection operator for lateral position \mathbf{x}_k being represented by the k th row of \mathbf{R} . According to equations A-1a and A-1b, unbiased estimation of \mathbf{R} requires uncommitted, i.e., data-driven, knowledge of \mathbf{W} (velocity problem). The first examples of complicated processing algorithms that are derived using the same uncommitted inversion formalism include surface-related multiples removal (Berkhout, 1982; Verschuur, 1991; Verschuur et al., 1992; Berkhout and Verschuur, 1997), elastic-reflectivity estimation (Berkhout, 1982; de Bruin et al., 1990), controlled illumination (Berkhout, 1982; Rietveld and Berkhout, 1994; Rietveld, 1995), and CFP technology (Berkhout and Verschuur, 1997; Thorbecke, 1997).

APPENDIX B

SURFACE-RELATED MULTIPLES REMOVAL BY CONVOLUTION AND CORRELATION

Figure B-1 shows the flow diagrams for surface-related multiples removal. Figure B-1a represents the surface-related multiples-elimination process in the convolution mode (SRME1), in which multiples are predicted by adding one round trip. The predicted multiples subsequently are subtracted from the input data. In the next iteration, the output of the SRME1 process is used as an improved multiples-prediction operator. Figure B-1b represents the multiples-removal procedure in the correlation mode. Using an estimate of the data without surface-related multiples — e.g., the output of the SRME1 process — a focal transformation is carried out, meaning that one round trip is removed. This focuses all the primaries into the area around the origin, as well as transforms first-order multiples into primaries and higher-order multiples into lower-order multiples. In the focal domain, a separation process (indicated as “bifocal imaging” in Figure B-1b) is carried out, preferably in the τ - p domain, yielding the focused primaries. The unfocused primaries are obtained by inverse focal transformation. In an iteration procedure, the newly obtained primaries can be used as an improved focal operator. Thus, the output of the convolution mode (SRME1) will serve as the estimated primary response, which serves again as operator for the focal transform in the correlation mode (SRME2), resulting in an improved primary estimate (Figure B-1c). Note that if an adaptive subtraction in the focal domain (equation 11d) is applied, a least-squares estimate of surface operator \mathbf{A} becomes available as well, which can be used in a new SRME1 process for the next iteration of SRME1 + SRME2 (Figure B-1d).

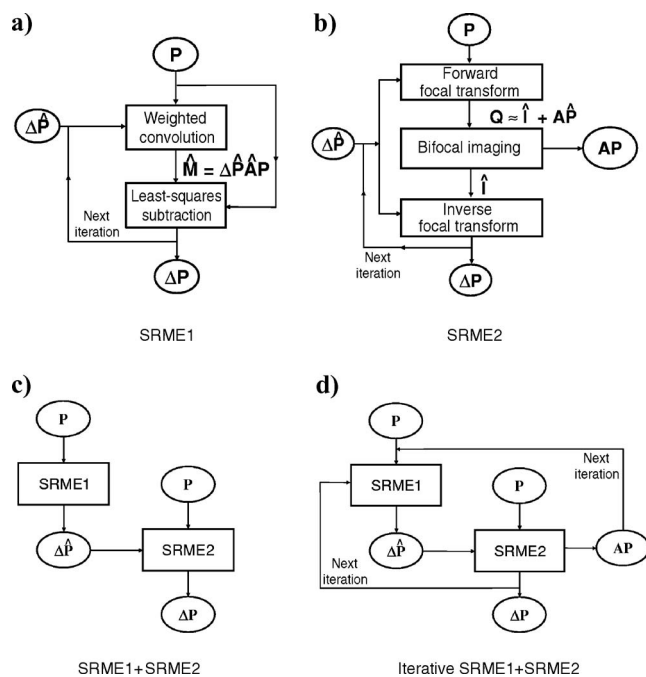


Figure B-1. Flow for surface-related multiple elimination in the convolution mode (a) and in the correlation mode (b). It is proposed that the two methods be used in combination. The output of the convolution mode will serve as the operator for the focal transform in the correlation mode (c). This combination also can be applied iteratively (d).

REFERENCES

- Berkhout, A. J., 1982, Seismic migration, imaging of acoustic energy by wave field extrapolation, A: Theoretical aspects: Elsevier.
- , 1992, Areal shot record technology: *Journal of Seismic Exploration*, **1**, 251–264.
- , 1993, A unified approach to acoustical reflection imaging, part 1: The forward model: *Journal of the Acoustical Society of America*, **93**, 2005–2017.
- , 1997, Pushing the limits of seismic imaging, part I: Prestack migration in terms of double dynamic focusing: *Geophysics*, **62**, 937–953.
- , 2003, Multiple removal: New opportunities: Annual International Meeting, EAGE, Expanded Abstracts.
- Berkhout, A. J., and D. J. Verschuur, 1995, Migration of multiple reflections: 57th Annual International Meeting, EAEG, Expanded Abstracts.
- , 1997, Estimation of multiple scattering by iterative inversion, part I: Theoretical considerations: *Geophysics*, **62**, 1586–1595.
- , 2003, Transformation of multiples into primary reflections: 73rd Annual International Meeting, SEG, Expanded Abstracts, 1925–1928.
- , 2005, Removal of internal multiples with the common-focus-point (CFP) approach: Part 1 — Explanation of the theory: *Geophysics*, **70**, V45–V60.
- Berkhout, A. J., D. J. Verschuur, and R. Romijn, 2004, Reconstruction of seismic data using the focal transformation: 74th Annual International Meeting, SEG, Expanded Abstracts, 1993–1996.
- Claerbout, J. F., 1968, Synthesis of a layered medium from its acoustic transmission response: *Geophysics*, **33**, 264–269.
- de Bruin, C. G. M., 1991, Linear AVO inversion by prestack depth migration: Ph.D. thesis, Delft University of Technology.
- de Bruin, C. G. M., C. P. A. Wapenaar, and A. J. Berkhout, 1990, Angle-dependent reflectivity by means of prestack migration: *Geophysics*, **55**, 1223–1234.
- Guittou, A., 2002, Shot-profile migration of multiple reflections: 72nd Annual International Meeting, SEG, Expanded Abstracts, 1296–1299.
- Guittou, A., and D. J. Verschuur, 2004, Adaptive subtraction of multiples using the L1-norm: *Geophysical Prospecting*, **52**, 27–38.
- Hampson, D., 1986, Inverse velocity stacking for multiple elimination: *Journal of the Canadian Society of Exploration Geophysicists*, **22**, 44–55.
- Herrmann, P., T. Mojesky, M. Magasan, and P. Hugonnet, 2000, De-aliased, high-resolution Radon transforms: 70th Annual International Meeting, SEG, Expanded Abstracts, 1953–1956.
- Ikelle, L. T., and L. Amundsen, 2002, Acquisition processing — Noniterative multiple attenuation methods: Linear inversion solutions to nonlinear inverse problems: *The Leading Edge*, **21**, 350–356.
- Jakubowicz, H., 1998, Wave equation prediction and removal of interbed multiples: 68th Annual International Meeting, SEG, Expanded Abstracts, 1527–1530.
- Kelamis, P. G., and D. J. Verschuur, 2000, Surface-related multiple elimination on land seismic data—Strategies via case studies: *Geophysics*, **63**, 719–734.
- Kelamis, P. G., D. J. Verschuur, K. E. Erickson, R. L. Clark, and R. M. Burnstad, 2002, Data-driven internal multiple attenuation — Applications and issues on land data: 72nd Annual International Meeting, SEG, Expanded Abstracts, 2035–2038.
- Miley, M. P., J. Paffenholz, K. Hall, and S. Mitchell, 2001, Optimizing surface-related multiple elimination on a synthetic subsalt data set: 71st Annual International Meeting, SEG, Expanded Abstracts, 1277–1280.
- Muijs, R., K. Holliger, and J. O. A. Robertsson, 2005, Prestack depth migration of primary and surface-related multiple reflections: 75th Annual International Meeting, SEG, Expanded Abstracts, SPMUL2.4.
- Nekut, A. G., and D. J. Verschuur, 1998, Minimum energy adaptive subtraction in surface-related multiple elimination: 68th Annual International Meeting, SEG, Expanded Abstracts, 1507–1510.
- Reiter, E. C., M. N. Toksoöz, T. H. Kebo, and G. M. Purdy, 1991, Imaging with deepwater multiples: *Geophysics*, **56**, 1081–1086.
- Rickett, J., and J. F. Claerbout, 1999, Acoustic daylight imaging via spectral factorization: *Heliophysics and reservoir monitoring: The Leading Edge*, **18**, 957–960.
- Rietveld, W. E. A., 1995, Controlled illumination in prestack seismic migration: Ph.D. thesis, Delft University of Technology.
- Rietveld, W. E. A., and A. J. Berkhout, 1994, Determination of macro models for prestack migration: Part 2, estimation of macro boundaries: 64th Annual International Meeting, SEG, Expanded Abstracts, 1334–1337.
- Robinson, E. A., 1957, Predictive decomposition of seismic traces: *Geophysics*, **22**, 767–778.
- Robinson, E. A., and S. Treitel, 1980, *Geophysical signal analysis*: Prentice-Hall, Inc.
- Schuster, G. T., J. Yu, J. Sheng, and J. Rickett, 2004, Interferometric/daylight seismic imaging: *Geophysical Journal International*, **157**, 838–852.
- Spitt, S., 2000, Model-based subtraction of multiple events in the frequency-space domain: 70th Annual International Meeting, SEG, Expanded Ab-

- stracts, 1969–1972.
- Sun, Y., 2001, Migrating multiples and primaries in CDP data by crosscorrelation migration: 71st Annual International Meeting, SEG, Expanded Abstracts, 1297–1300.
- Thorbecke, J. W., 1997, Common focus point technology: Ph.D. thesis, Delft University of Technology.
- Trad, D. O., T. Ulrych, and M. Sacchi, 2003, Latest views of the sparse Radon transform: *Geophysics*, **68**, 386–399.
- Verschuur, D. J., 1991, Surface-related multiple elimination: An inversion approach: Ph.D. thesis, Delft University of Technology.
- , 1992, Surface-related multiple elimination in terms of Huygens' sources: *Journal of Seismic Exploration*, **1**, 49–59.
- Verschuur, D. J., and A. J. Berkhout, 1997, Estimation of multiple scattering by iterative inversion, part II: Practical aspects and examples: *Geophysics*, **62**, 1596–1611.
- Verschuur, D. J., A. J. Berkhout, and C. P. A. Wapenaar, 1992, Adaptive surface-related multiple elimination: *Geophysics*, **57**, 1166–1177.
- Wapenaar, C. P. A., J. W. Thorbecke, and D. Draganov, 2004, Relations between reflection and transmission responses of three-dimensional inhomogeneous media: *Geophysical Journal International*, **156**, 179–194.
- Weglein, A. B., F. A. Gasparotto, P. M. Carvalho, and R. H. Stolt, 1997, An inverse scattering series method for attenuating multiples in seismic reflection data: *Geophysics*, **62**, 1975–1989.
- Youn, O. K., and H. W. Zhou, 2001, Depth imaging with multiples: *Geophysics*, **66**, 246–255.